Characterization of deposited Ti-doped lithium aluminium hydride thin film using dip coating method

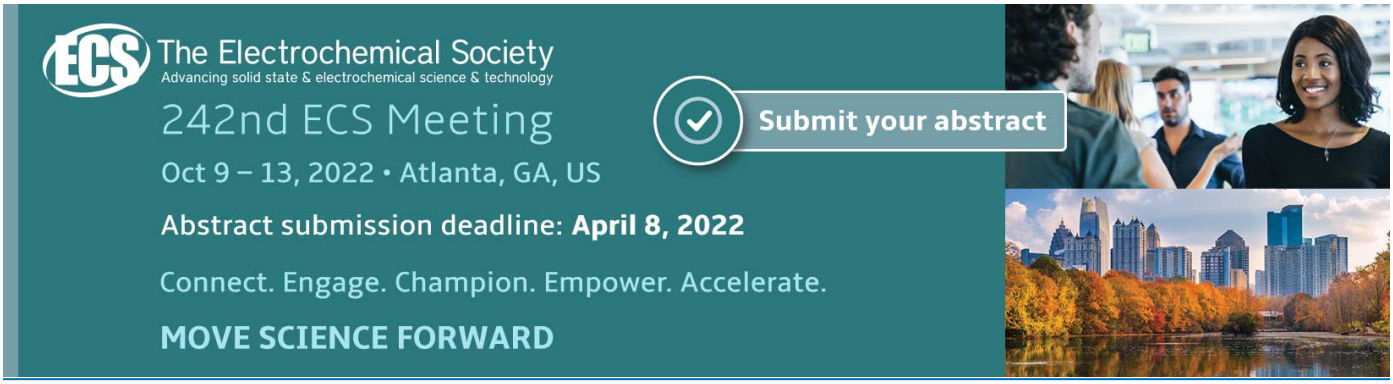

Characterization of deposited Ti-doped lithium aluminium hydride thin film using dip coating method

C. Chowarot[1], V. Siriwongrungsona[1,*], J. Hongrapipat[2], S. Pang[3] and M. Messner[2]

[1] College of Advanced Manufacturing Innovation, King Mongkut's Institute of Technology Ladkrabang, Bangkok 10520, Thailand
[2] Gussing Renewable Energy (Thailand) Co., Ltd., Bangkok 10500, Thailand,
[3] Department of Chemical and Process Engineering, University of Canterbury, Christchurch 8041, New Zealand

*Corresponding Author's E-mail: vilailuck.si@kmitl.ac.th

Abstract. Lithium aluminium hydride ($LiAlH_4$) is an outstanding complex metal hydride as a hydrogen storage material. The hydrogen storage capacity of $LiAlH_4$ is about 5-7 wt%. In this study, $LiAlH_4$ concentration of 20 g/l doped with various titanium (Ti) concentration by dip coating method was examined. The titanium dioxide (TiO_2) powder at 10 mol %, 25 mol % and 40 mol % was used as the Ti source. Instruments used to analyze Ti-doped $LiAlH_4$ were X-ray powder diffraction (XRD) and scanning electron microscope (SEM). XRD was used for phase and crystallite size analysis and SEM was used for surface morphology investigation. The experimental results reveal that at the $LiAlH_4$ concentration of 20 g/l with 40 mol% of TiO_2, the smallest crystallite size with rather dense surface was shown. The small crystallite size can improve the desorption of hydrogen from its surface area. Therefore, the addition of titanium might be advantageous in improving the hydrogen storage efficiency of $LiAlH_4$.

1. Introduction

Hydrogen is a clean energy and classified as non-toxic gas. When hydrogen is stored, it can be used and transported anywhere. Additionally, the hydrogen storage solves two main renewable energy problems i.e., the valorization of excess energy and a long-term clean energy storage system [1]. At present, the hydrogen storage technologies can be divided into 4 categories i.e., compressed hydrogen, liquid hydrogen, chemical hydrogen and solid-state hydrogen storage. The hydrogen storage improvement concerns about safety, reliability, compactability and low-cost with acceptable efficiency. The metal hydride in solid-state hydrogen storage development reveals many properties including hydrogen storage capacity, kinetics, cyclic behavior, toxicity, pressure and thermal response [2].

There are materials in solid-state hydrogen storage group. These are such as lithium aluminium hydride ($LiAlH_4$), sodium aluminium hydride ($NaAlH_4$), lithium amide and sodium borohydride ($NaBH_4$). The $LiAlH_4$ properties corresponding with the hydrogen storage improvement has the maximum hydrogen gravimetric density of around 10.6 wt% and the minimum desorption temperature of 180 °C.

For the solid-state hydrogen storage synthesis method, there were several methods including ball-milling, sputtering and electrophoretic deposition (EPD) [3]. For the high-energy ball-milling of $LiAlH_4$, good stability of the complex aluminohydride for up to 35 h was reported [4]. Additionally, the dehydrogenation kinetic of $LiAlH_4$ into Li_3AlH_6 and LiH was analyzed by ball milling. A relationship between crystallite size and dehydrogenation kinetics of $LiAlH_4$ and Li_3AlH_6 were found. On the

contrary, the kinetic of LiH was independent of crystallite size. This can be implied that the reaction of LiH is limited by the intrinsic kinetics while the reaction of $LiAlH_4$ and Li_3AlH_6 is limited by mass transfer [5]. The adsorption-desorption of Pd/Mg films formation in various sputtering conditions through the changing the RF coil has been investigated. They found that the dehydriding temperature decreased with decreasing degree of crystallization [6]. The hydrogen storage capacity of nickel particles deposited on carbon nanotubes using EPD was studied. The results showed that with increasing the number of cycles at a constant current, the capacity was increased and reached a constant value. Additionally, the post-annealing led to higher strength of the surface [3].

The titanium shows its important role in the hydrogen storage capacity. This is because small quantity of proper titanium catalyst can speed up the reaction, which makes it a suitable catalyst for practical hydrogen storage applications [7]. Additionally, the effort of $LiAlH_4$ production has been investigated by doping of $LiAlH_4$ with different Ti precursors such as titanium (Ti), titanium dioxide (TiO_2), and titanium chloride ($TiCl_3$) [8]. TiO_2 is of interest in this study because of its higher short-term stability than Ti and $TiCl_3$ with comparable desorption temperature and activation energy [8].

In this paper, the amount of TiO_2 at 0 mol%, 10 mol%, 25 mol % and 40 mol %mixed with the $LiAlH_4$ at the concentration of 20 g/l using the dip coating method was studied. TiO_2 was used as the Ti source. The dip-coating method is a simple method and low development cost for higher hydrogen storage capacity.

2. Materials and methods

2.1 Chemicals and substrates

All chemicals used in this study are $LiAlH_4$ powder grade (95% reagent), titanium dioxide nanopowder (anatase, 99.5% reagent) and dimethyl ether (DME) (99% or above solvent) supplied from Sigma-Aldrich. Before used, the solvent was pre-dried with 3A molecular sieve. Glass slide substrates (25x25 mm^2) were used. Each substrate was cleaned by acetone followed by isopropanol (IPA). The substrates were heated at 105°C for at least 1 hour before dip coating in a controlled humidity and inert nitrogen atmosphere.

2.2 Methods

2.2.1 Precursor and thin film preparation

The precursor preparation and thin film coating process of $LiAlH_4$ doped with TiO_2 is shown in Figure 1. $LiAlH_4$ powder of 1.0 g was mixed with 0 mol%, 10 mol%, 25 mol% and 40 mol% of TiO_2 in a 50 ml Pyrex bottle to the $LiAlH_4$ concentration of 20 g/l with TiO_2 doping. The solution preparation was operated under the controlled humidity and nitrogen atmosphere. Additionally, it was ultrasonicated for 1 hour and stirred with magnetic stirrer for 30 min. The dip coating was conducted under the same controlled humidity and inert nitrogen atmosphere for 10 times. The next dip coating was 3 s after the previous dip-coating.

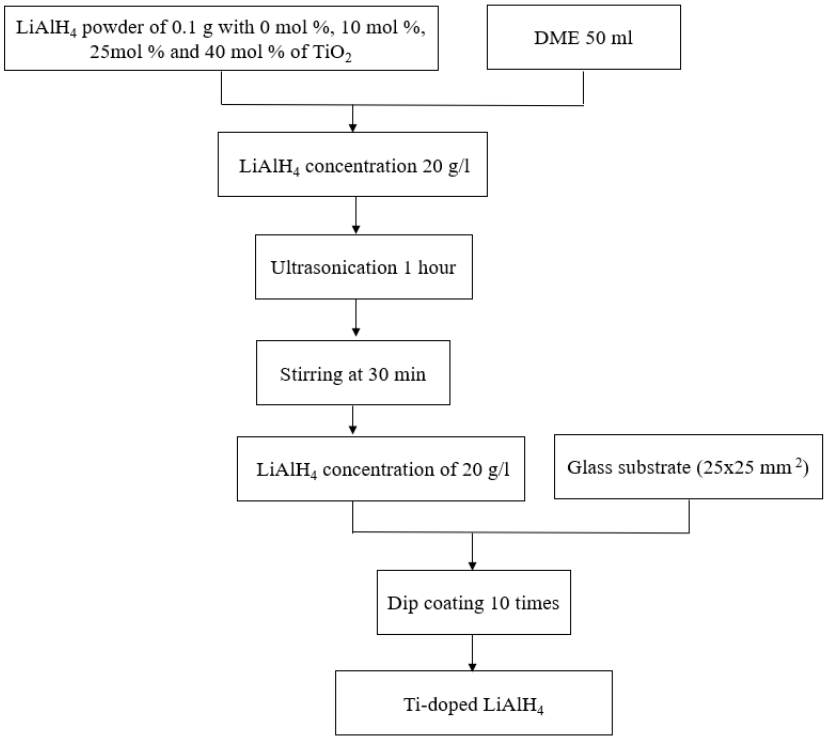

Figure 1. The process of Ti-doped $LiAlH_4$ thin film preparation under the controlled humidity and inert nitrogen atmosphere.

2.2.2 $LiAlH_4$ thin film analysis

Scanning electron microscope (SEM) was used for surface analysis. The SEM used is Carl Zeiss the EVO® HDat 20 kV and magnification at 1000x. The phase of the Ti-doped $LiAlH_4$ thin films were characterized using X-ray diffraction (XRD). The XRD was operated at 30 mA and 40 kV with a graphite - monochromated Cu Kα radiation (λ = 1.54180 A°), X-ray tube with Cu, velocity of 0.02 ° per step (2 min^{-1}) and scan axis at 10 deg – 80 deg with Theta/2-Theta. The crystallite size were calculated from Scherrer equation as writtten in Equation 1:

$$D = \frac{K\lambda}{\beta\cos\theta} \quad (1)$$

Where D is the crystallite size, K is the Scherrer constant (0.9), λ is wavelength of the X-ray source (0.15406 nm), β is the full width at half maximum (FWHM) at the peak solution and θ is the Bragg angle by 11.855° for lithium aluminium hydride ($LiAlH_4$) ,19.035° for lithium hexahydroaluminate (Li_3AlH_6) and anatase titanium dixoide **(**TiO_2**)** for 12.15°. The $LiAlH_4$, Li_3AlH_6 and TiO_2 peaks were identified by JCPDS file No. 12-0437, 47-1157 and 84-1286, respectively.

3. Results and discussion

3.1 Phase and crystallite size

As can be seen in Figure 2, the peak intensity of Ti-doped $LiAlH_4$ (002) peak at 23.71° is higher than any other peaks. The peak intensity of $LiAlH_4$ are (002), (031), (013) and (231) peaks and there are three peak intensity of Li_3AlH_6, which is (113), (302) and (401) peak. When considering the calculated crystallite size as summarized in Table 1, the crystallite size with the use of TiO_2 concentrations of 0 mol%, 10 mol%, 25 mol% and 40 mol% are 86.20 nm, 75.42 nm, 52.60 nm and 34.22 nm, respectively. It is obvious that the XRD highest peak and minimum crystallite size were obtained at the $LiAlH_4$ concentration of 20 g/l with 40 mol% TiO_2. This can be implied that the doping with Ti enhances the kinetics of hydrogen storage [10]. The kinetics of hydrogen loading and releasing are a function of the

crystallite size. Moreover, it was found that the hydrogenation efficiency increases with the decreasing crystallite size [10]. This is because the smaller crystallite size was found to improve the desorption kinetics of hydrogen storage from the higher surface area [11].

Table. 1 Calculated crystallite size of Ti-doped $LiAlH_4$ thin film at various TiO_2 concentrations.

TiO_2 concentration (mol %)	0%	10%	25%	40%
Crystallite size (nm)	86.20	75.42	52.60	34.22

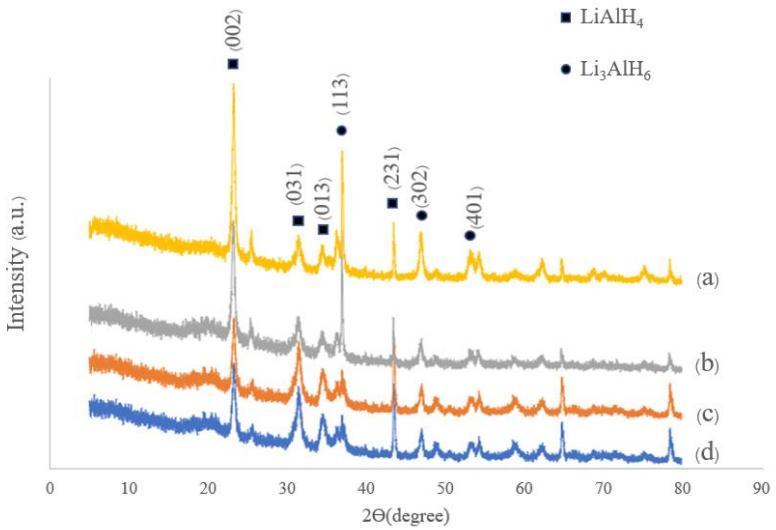

Figure 2. XRD patterns of the deposited Ti-doped $LiAlH_4$ thin film at the $LiAlH_4$ concentration of 20 g/l and TiO_2 concentrations of (a) 0 mol%, (b) 10 mol%, (c) 25 mol% and (d) 40 mol%.

3.2 Surface morphology

The SEM images in Figure 3 show the surface morphology of Ti-doped $LiAlH_4$ at the concentration of 20 g/l with various TiO_2 concentrations. For the $LiAlH_4$ without TiO_2, cracks and holes on the surface was found. Less cracks and smaller holes were observed with the use of the Ti-doped $LiAlH_4$ with TiO_2 at 10 mol% concentration. The Ti-doped $LiAlH_4$ with 40 mol% TiO_2 concentration has rather dense surface without holes. From such a surface morphology observation, it can be implied that the dense surface without any cracks was improved with the incorporation of increasing amount of the TiO_2 [12,13]. This is because the amount of TiO_2 reduces the solvent evaporation rate [14]. In this study, the optimal condition is then the deposition of the Ti-doped $LiAlH_4$ with the 40 mol% TiO_2 concentration.

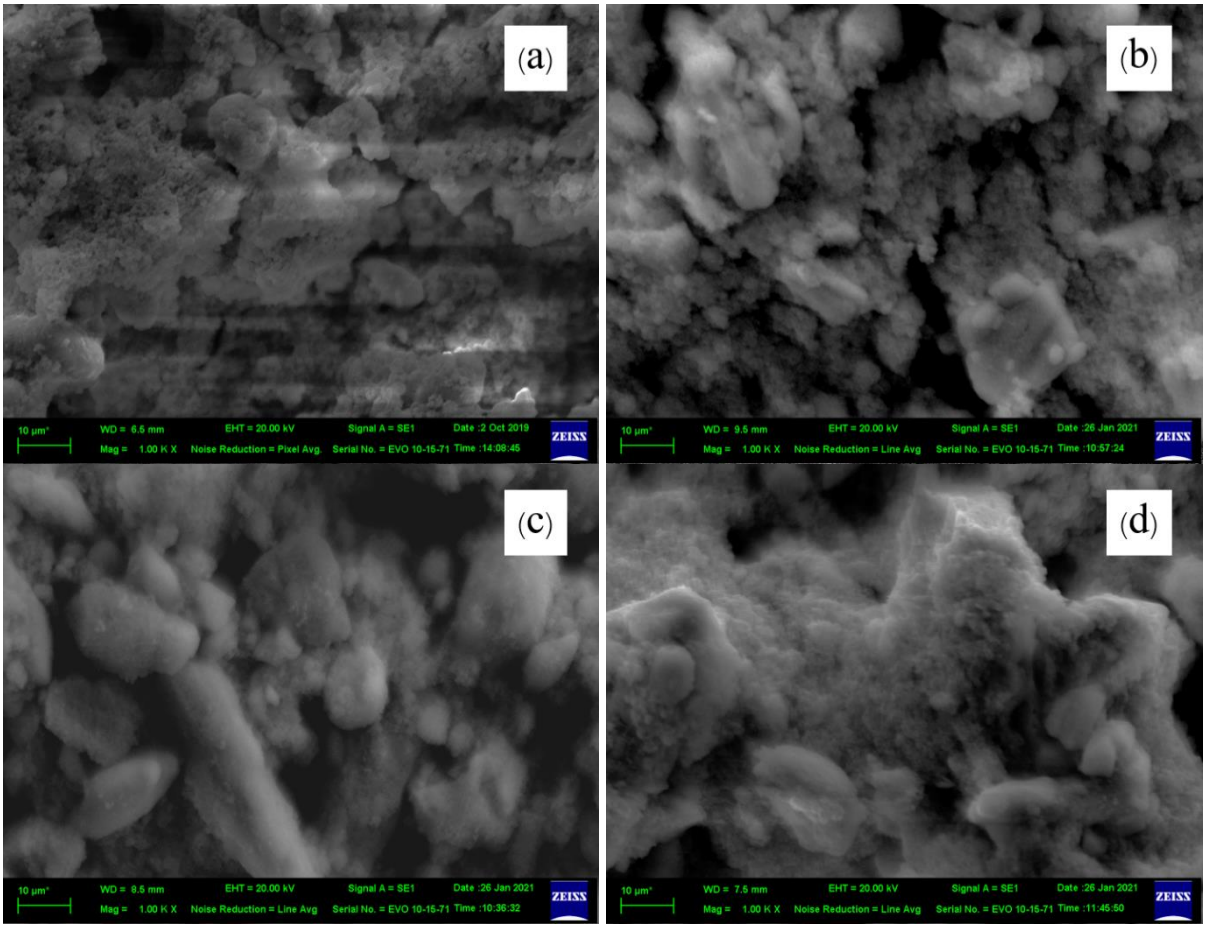

Figure 3. SEM images (1000x) of $LiAlH_4$ concentration of 20 g/l with the different TiO_2 concentrations: (a) 0 mol%, (b) 10 mol%, (c) 25 mol% and (d) 40 mol%.

4. Conclusions

The dip coating method was applied to fabricate the Ti-doped $LiAlH_4$ at the concentration of 20 g/l with the various TiO_2 concentrations of 0 mol%, 10 mol %, 25 mol% and 40 mol%. The $LiAlH_4$ (002) peak is the most intense peak in the XRD pattern. When considering the crystallite size corresponding with (002) peak, the crystallite size at 0 mol%, 10 mol %, 25 mol% and 40 mol% TiO_2 concentration were 86.20 nm, 75.42 nm, 52.60 nm and 34.22 nm, respectively. The small crystallite size improved the kinetics of hydrogen storage. Therefore, the Ti-doped $LiAlH_4$ at the TiO_2 concentration of 40 mol% is expected to produce the largest amount of hydrogen in this study. Moreover, the SEM also showed the dense surface without any cracks of Ti-doped $LiAlH_4$ at the TiO_2 concentration of 40 mol%. Therefore, it might be suggested that increasing the amount of Ti doping increase the efficiency of hydrogen storage.

Acknowledgements

The authors would like to thank the College of Advanced Manufacturing Innovation, King Mongkut's Institute of Technology Ladkrabang, Bangkok, for SEM and XRD supports. The financial support from the Research and Researchers for Industries (RRI), under the Thailand Science Research and Innovation (TSRI) and Gussing Renewable Energy (Thailand) Co., Ltd, Grant Number MSD60I0102 are appreciated.

References

[1] Yodpradit K 2020 *Role of hydrogen* (Thailand: King Mongkut's University of Technology North Bangkok)
[2] Sakintuna B, Lamari-Darkrim F and Hirscher M 2007 Metal hydride materials for solid hydrogen storage: A review *J. Hydrog. Energy.* **32** pp 1121-40
[3] Mohammadi M, Khoshnevisan B and Varshoya Sh 2016 Electrochemical hydrogen storage in EPD made porous Ni-CNT electrode *J. Hydrog. Energy.* **41** pp 10311-5
[4] Balema V P, Pecharsky V K and Dennis KW 2000 Solid state phase transformations in $LiAlH_4$ during high-energy ball-milling *J. Alloys Compd.* **313** pp 69-74
[5] Andreasen A, Vegge T and Pedersen A S 2005 Dehydrogenation kinetics of as-received and ball-milled $LiAlH_4$ *J. Solid State Chem.* **178** pp 3672-8
[6] Higuchi K, Kajioka H, Toiyama K, Fujii H, Orimo S and Kikuchi Y 1999 In situ study of hydriding–dehydriding properties in some Pd/Mg thin films with different degree of Mg crystallization *J. Alloys Compd.* **293** pp 484-9
[7] Chaudhuri S and Muckerman T J 2005 First-principles study of Ti-Catalyzed hydrogen chemisorption on an Al Surface: A critical first step for reversible hydrogen storage in $NaAlH_4$ *J. Phys. Chem. B.* **109** pp 6952-7
[8] Amama B P, Grant T J, Shamberger J P, Voevodin A A and Fisher S T 2012 Improved dehydrogenation properties of Ti-doped $LiAlH_4$: Role of Ti precursors *J. Phys. Chem. C.* **41** pp 21886-94
[9] Gross K J, Carrington K R, Barcelo S, Karkamkar A, Purewal J, Ma S, Hong-cai Z, Dantzer P, Ott K, Burrell T, Semeslberger T, Pivak Y, Dam B and Chandra D 2012 Recommended best practices for the characterization of storage properties of hydrogen storage materials (Washington, DC)
[10] Milcius D, Pranevicius L, Templier C, Bobrovaite B and Barnackas I 2006 Role of grain boundaries in the mechanism of plasma Hydrogenation of nanocrystalline Mg-Al Films *AIP Conf. Proc.* **837** p 22
[11] Li Z, Li P, Wan Q, Zhai F, Liu Z, Zhao K, Wang L, Lu S, Zou L, Qu X and Volinsky A A 2013 Dehydrogenation improvement of $LiAlH_4$ catalyzed by Fe_2O_3 and Co_2O_3 nanoparticles *J. Phys. Chem. C.* **17** pp 18343–52.
[12] Ismail M, Zhao Y, Yu X B, Nevirkovets I P and Dou S X 2011 Significantly improved dehydrogenation of $LiAlH_4$ catalyzed with TiO_2 nano powder *J. Hydrog. Energy.* **36** pp 8327 - 34
[13] Liu S H, Zhang Y, Sun L X, Zhang J, Zhao J N, Xu F and Huang F.L 2010 The dehydrogenation performance and reaction mechanisms of Li_3AlH_6 with TiF_3 additive *J. Hydrog. Energy.* **35** pp 4554 – 61
[14] Monica S, Johannes M, Steffen B. F, Moritz W, Norbert W and Erin K 2018 Suppressing Crack Formation in Particulate Systems by Utilizing Capillary Forces *ACS Appl Mater Interfaces.* **9** pp 11095–11105